Deep Learning Based Semi-Supervised Control for Vertical Security of Maglev Vehicle With Guaranteed Bounded Airgap

Yougang Sun, *Member, IEEE*, Junqi Xu, Han Wu, Guobin Lin, and Shahid Mumtaz, *Senior Member, IEEE*

***Abstract*— The vertical security problem of maglev train is challenging for nonlinearity, external disturbances, unmeasurable airgap velocity and constrained output. To solve this problem, a semi-supervised controller based on deep belief network (DBN) algorithm is proposed in the presence of unknown external disturbances. Firstly, the extended state observer (ESO) is designed to ensure fast convergence of observation errors with high enough estimation precision. An output-constrained controller is designed by backstepping method, and the estimated value of ESO is introduced to ensure that the output airgap is constrained within a bounded range. Then, the stability of this method is proved based on the symmetric Barrier Lyapunov function. Subsequently, a semi-supervised controller is presented based on DBN algorithm and the output-constrained controller. The numerical simulation results show that this method can effectively deal with unmeasurable airgap velocity and generalized external disturbances, and guarantee the vertical security with output airgap within a bounded range. Finally, experiments are implemented on a full-scale maglev vehicle and the experimental results demonstrate that the developed deep learning controller can ensure the vertical security.**

***Index Terms*— Extended state observer, intelligent control, nonlinear dynamics, state constrains, vertical security.**

I. Introduction

MAGLEV vehicle is a new type of rail transit tools [1]–[3]. Different from the ordinary wheel-rail train, the maglev vehicle mainly relies on electromagnetic force to levitate the body above the track to run [4], [5]. Because there is no contact between the car body and the track, the friction between the vehicle body and the track can be neglected so as to improve the limited value of train speed. In practice, the value of suspension airgap is not arbitrary. Because of the existence of physical constraints, the suspension airgap can only change in the range of 0-16 mm. Once the airgap great than 16 mm, the suspension chassis of maglev train collides with the track (called "rail smashing") or less than 0 mm, the suspension electromagnet sucks with the track (called "magnet smashing"). The current control algorithm cannot guarantee the bounded suspension airgap. In actual operation, there will be rail smashing or magnet smashing, which seriously affects the vertical security of maglev vehicle. In addition, in the general magnetic suspension control system, the airgap value can be obtained by eddy current sensor, and the vertical acceleration of electromagnet can also be obtained by acceleration sensor, but the airgap change velocity value cannot be measured directly [6], [7]. If the airgap is differentiated to obtain the velocity, it is easy to introduce great disturbance at high frequencies. If the acceleration is integrated to obtain the airgap change velocity, the system is easy to integrate saturation at low frequency, which results in large error. Therefore, it is necessary to design a state observer to estimate the airgap velocity. In fact, observers and controllers affect each other in the system. How to ensure the security of the coupled system with the designed observers and controllers has been seldom studied.

As a typical open-loop unstable, strong nonlinear and susceptible to external disturbance system, the research of control algorithm of maglev train has been very challenging. At present, most commercial maglev trains adopt mature linear control theory. In the design of controller and stability analysis, the system is often linearized near the equilibrium point. But when the system state is far from the equilibrium point, the control effect will be greatly deteriorated. How to design a nonlinear controller and simultaneously solve the problem of airgap state limitation and airgap velocity unmeasurable is a tough problem in the control system of maglev train at present. The back-stepping control method or improved back-stepping method is very powerful tool to deal with nonlinear system [8]–[10]. Michino *et al.* [11] introduced two different virtual filters, and a high-gain adaptive output feedback controller is designed using backstepping strategy. Finally, the high-gain adaptive output feedback controller is applied to the magnetic suspension system, and satisfactory tracking results are obtained. Liu *et al.* [12] proposed an adaptive control

Manuscript received June 4, 2020; revised September 9, 2020 and October 27, 2020; accepted November 23, 2020. This work was supported in part by the National Natural Science Foundation of China under Grant 51905380 and Grant 51805522 and in part by the China Postdoctoral Science Foundation under Grant 2019M651582 and Grant 2020T130475. The Associate Editor for this article was A. Jolfaei. *(Corresponding authors: Junqi Xu; Han Wu.)*

Yougang Sun is with the Institute of Rail Transit, Tongji University, Shanghai 201804, China, and also with the National Maglev Transportation Engineering R&D Center, Tongji University, Shanghai 201804, China (e-mail: 1989yoga@tongji.edu.cn).

Junqi Xu and Guobin Lin are with the National Maglev Transportation Engineering R&D Center, Tongji University, Shanghai 201804, China (e-mail: xujunqi@tongji.edu.cn; linguobin@tongji.edu.cn).

Han Wu is with the Key Laboratory for Mechanics in Fluid Solid Coupling Systems, Institute of Mechanics, Chinese Academy of Sciences, Beijing 100190, China (e-mail: wuhan@imech.ac.cn).

Shahid Mumtaz is with the Instituto de Telecomunicações, 3810-193 Aveiro, Portugal (e-mail: dr.shahid.mumtaz@ieee.org).

Digital Object Identifier 10.1109/TITS.2020.3045319

strategy based on backstepping method for nonlinear magnetic suspension system with disturbance, which can effectively improve its anti-disturbance ability. Saikia *et al.* [13] combined the backstepping method with sliding mode control method and applied it to the magnetic suspension control system. The impulse signal is simulated as disturbance, and the simulation results show the proposed controller can track the target trajectory more accurately. The above works are done under the condition that all states are known. However, in practice, some states in the magnetic suspension system cannot be measured directly or mismeasurement because of sensor fault. It is necessary to design a state observer to estimate these state values which cannot be measured directly. Recently, the disturbance estimation issues have attracted a lot of research attentions [14]–[16]. Liu [17] discussed the state observer in detail, and estimated the unmeasurable state variables by state reconstruction. The proposed state observer lays a foundation for the subsequent development of other forms of state observers. The extended state observer (ESO) can observe the unmeasurable state and external disturbance in the system. It is an important part of the non-linear control technology such as active disturbance rejection controller [18], [19]. It is noteworthy that ESO is an effective and practical method for estimating unknown states or uncertainties [20]. He [21] proposed a new bearingless suspension system based on ESO. Using ESO to estimate disturbances, a mathematical model was established. Zhao [22] proposed a novel control method for a two-joint manipulator system driven by pneumatic artificial muscle. A nonlinear ESO is developed to estimate the disturbance and state of the system. Sun [23] proposed an adaptive neuro-fuzzy sliding mode controller. Simulation and experimental results show that the proposed robust controller can cope with the disturbance and parameter perturbations effectively. Wai *et al.* [24] proposed an adaptive observer to estimate the airgap change velocity and passed it to the suspension controller. Chen *et al.* [25] used the linear Kalman filter algorithm to design the observer, and obtained the state observation value of vehicle suspension vibration by coordinate inverse transformation. Wang *et al.* [26] designed speed state observer based on second-order sliding mode for linear motor control of medium and low speed maglev vehicle system. Xu *et al.* [27] proposed a hybrid flux density observer for maglev vehicles. Sun [28] proposes an on-line estimation method of periodic interference based on repetitive learning, which is applied in magnetic suspension system. These observers or on-line estimation algorithms provide many new ideas for the state observer of maglev train, but neglect the limitation of airgap state output of maglev train.

Output constraints refer to the fact that the output of the actual system cannot exceed a certain range [29]. The general Lyapunov function used in traditional controller design can only make it stable without restricting the output value to a certain range due to the lack of self-constraints. At present, some scholars have proposed barrier Lyapunov function (BLF). This Lyapunov function can set constraints. When the constraints are closer to the critical constraints, the value of its function tends to be infinite, thus constraining the constraints to the interval. Tee *et al.* [30] proposed the control design of SISO nonlinear systems with strict feedback form with output constraints. Asymmetric barrier Lyapunov function is designed to relax the requirement of initial value. The simulation results of symmetric barrier Lyapunov function, asymmetric barrier Lyapunov function and controller design based on quadratic Lyapunov function show that barrier Lyapunov function is better than quadratic Lyapunov function. The adaptive control method has also attracted much attention [31]–[33]. Xu *et al.* [33] proposed an adaptive robust control method for the suspension control of a nonlinear maglev train with state constraints. A three-step state transition method is designed to transform the maglev train into an interconnected uncertain system. At the same time, in order to prevent collision, the airgap between the suspension electromagnet and the guideway is limited to a specific range, but the problem that the airgap change speed is unmeasurable in practice is neglected. Moreover, the study on the combination of deep learning algorithms [34]–[36] and advanced control method to deal with complex control problems of maglev system is less. Deep learning originated from the research of neural network, which can be understood as deep neural network. Through it, deep feature representation can be obtained, which can avoid the complexity of manual feature selection and dimension disaster of high-dimensional data. At present, the basic models of deep learning include Deep belief network (DBN) [37], Stacked auto encoders (SAE) [38], Convolutional neural networks (CNN) [39] and Recurrent neural networks (RNN) [40]. In order to overcome the shortcomings of the traditional neural network, such as slow convergence and easy convergence to the local optimum, this paper uses DBN to design the controller, which is more convenient to learn and deal with the uncertainty encountered of the maglev vehicle in the actual situation.

Considering the physical limitation of airgap between the suspension electromagnet and the track, the unmeasurable airgap velocity and unknown external disturbance of maglev train, an output-constrained maglev train backstepping control strategy based on ESO is proposed. The strategy introduces the estimation of airgap velocity and external disturbance by the ESO into the controller. The suspension controller is designed by combining the output constraints with the estimation of the extended state observer. Then the stability analysis is carried out based on the symmetric Barrier Lyapunov function. Next, the deep learning semi-supervised controller based on deep belief network (DBN) algorithm is developed. In order to prove the validity and reliability of the developed vertical security control method, numerical simulation is carried out according to the actual situation. Finally, the experimental verification is carried out through the experimental platform. The main contribution of this work is summarized as follows:

The main contribution of this work is summarized as follows:

1. The proposed controller can ensure the airgap to be always within a permitted range despite unmeasurable system state and external disturbances.

2. The deep belief network is utilized to learn the maglev control system, which is more effective to learn and deal with the uncertainties encountered in practice.

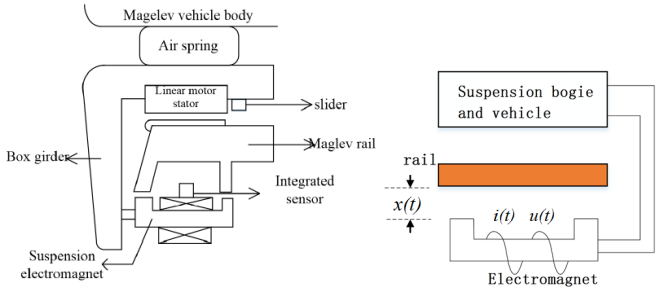

Fig. 1. Structure of maglev system.

3. Experimental results illustrate that the proposed method can achieve increased control performance than traditional method and airgap can constrained within the permitted range

The rest of this paper is structured as follows. In section 2, the mathematical model of maglev system is established and analyzed. Section 3 designs the extended state observer (ESO). Section 4 proposes a deep learning controller and stability analysis. Simulation and experiment results are provided in Section 5 and 6, respectively. Finally, the conclusions and future work directions are drawn in Section 7.

II. Vertical Dynamics and Security Analysis of Maglev Vehicle

A single module of the magnetic suspension system of the maglev train can be illustrated in Fig. 1. Based on Newton's law and Kirchhoff's law, the dynamic model of maglev system can be established as follows [23]:

$$\begin{cases} m\ddot{x} = mg - F(t) + \delta(t) \\ F(t) = \kappa \cdot \dfrac{i^2(t)}{x^2(t)} \\ Ri(t) + L\dfrac{di(t)}{dt} = u(t) \end{cases} \tag{1}$$

where $x(t), \dot{x}(t), \ddot{x}(t)$ represent the airgap, airgap velocity and acceleration between the suspension electromagnet and the track respectively; m represents the mass of the train; g is the gravitational acceleration; $F(t)$ denotes the electromagnetic force, κ is the electromagnetic force transmission coefficient determined by the effective area of the magnet and the turns number of the coil; $i(t)$ represents the excitation current, $u(t)$ denotes the voltage; R and L represent the resistance and inductance of the electromagnet respectively; $\delta(t)$ represents various disturbance forces in the vertical direction of the train.

To simplify the design, the disturbance force $\delta(t)$ is assumed to be a bounded function with period T as follows [28].

$$\delta(t) = \delta(t - T), \quad \delta(t) \le \delta_0 \le mg \tag{2}$$

For the maglev train system, the voltage $u(t)$ can be changed to adjust the current $i(t)$, thus changing the electromagnetic force $F(t)$ to make the train levitate stably at a reference height.

Remark 1: Airgap $x(t)$ is related to the safety of maglev train and will be limited to a range $(x_{\min}, x_{\max})$. If the airgap exceeds the range, it will cause rail or magnet smashing.

Definition 1: The nonlinear systems can be described as follows:

$$\dot{\mathbf{x}} = \mathbf{f}(\mathbf{x}), \quad \mathbf{x} \in R^n \tag{3}$$

where $\mathbf{x}$ denotes system state; $\mathbf{f}(\mathbf{x})$ represents nonlinear function.

The first linear approximation of (3) near the equilibrium point $\mathbf{x_0}$ can be reduced into:

$$\dot{\mathbf{x}} = \mathbf{A}(\mathbf{x_0})_{(\mathbf{x}-\mathbf{x_0})}, \quad \mathbf{x} \in R^n \tag{4}$$

where $\mathbf{A}(\mathbf{x_0})$ denotes a constant matrix. If $\mathbf{x_0}$ is an isolated singular point of a nonlinear system (3) and all eigenvalues of $\mathbf{A}(\mathbf{x_0})$ have non-zero real parts, then $\mathbf{x_0}$ is called a hyperbolic singular point of a nonlinear system (3).

The nonlinear systems (3) can be rewritten as below:

$$\dot{\mathbf{x}} = \mathbf{A}(\mathbf{x_0})(\mathbf{x} - \mathbf{x_0}) + \mathbf{O}(\mathbf{x} - \mathbf{x_0}), \quad \mathbf{x} \in R^n \tag{5}$$

Theorem 1: If $\mathbf{x_0}$ is a hyperbolic singularity of a nonlinear system (3), and the following condition is satisfied:

$$\lim_{\mathbf{x}\to\mathbf{x_0}} \left(\frac{\mathbf{O}(\mathbf{x} - \mathbf{x_0})}{|\mathbf{x} - \mathbf{x_0}|} \right) = 0 \tag{6}$$

Theorem1 is mainly to serve the subsequent stability analysis. With Theorem 1, the system (3) has the same topological structure as its corresponding linear system (5) at the isolated singular point $\mathbf{x_0}$ [41].

Remark 2: The vector field of the linearized system of hyperbolic nonlinear system at its equilibrium point is topologically equivalent to that of the original system near that point.

Remark 3: If the non-linear system and the linearized system are topologically equivalent at the equilibrium point, then the stability of the non-linear system near the equilibrium point can be determined by the linearized system.

According to theorem 1, the characteristics of the nonlinear magnetic suspension system can be analyzed by linear analysis method, which can ensure the accuracy of the analysis results under certain accuracy.

The linearized model of nonlinear magnetic suspension system (1) at equilibrium point $\mathbf{x_0}$ can be described as follows:

$$\dot{\mathbf{x}} = \mathbf{A_0}(\mathbf{x}_0)(\mathbf{x} - \mathbf{x}_0) + \mathbf{A_1}(u_m - u_0) + \mathbf{O}(\mathbf{x} - \mathbf{x}_0)^n \tag{7}$$

where

$$\mathbf{x_0} = (x_{ref}, 0, i_{ref}),$$

$$\mathbf{A_0} = \begin{bmatrix} 0 & 1 & 0 \\ \dfrac{P_x}{m} & 0 & -\dfrac{P_i}{m} \\ 0 & \dfrac{P_i}{L_{ref}} & -\dfrac{R}{L_{ref}} \end{bmatrix}, \quad \mathbf{A_1} = \begin{bmatrix} 0 \\ 0 \\ \dfrac{1}{L_{ref}} \end{bmatrix},$$

$$P_i = \frac{2\kappa i_{ref}}{m x_{ref}^2}, \quad P_x = \frac{2\kappa i_{ref}^2}{m x_{ref}^3}, \quad L_{ref} = \frac{2\kappa}{m x_{ref}}.$$

Through the Laplace transform, (7) can be rewritten as follows:

$$(ms^2 - P_x)\Delta x(s) = -P_i \Delta i(s) \tag{8}$$

$$\Delta u(s) = (R + L_{ref} s)\Delta i(s) - P_i s \Delta x(s) \tag{9}$$

Based on the (8) and (9), the transfer functions of the system can be obtained as follows:

$$G(s) = \frac{\Delta x(s)}{\Delta u(s)} = \frac{-P_i}{L_{ref} m s^3 + Rms^2 + (P_i^2 - L_{ref} P_x)s - RP_x} \quad (10)$$

Theorem 2: If the characteristic equation of the system is expressed as below:

$$a_n s^n + a_{n-1} s^{n-1} + \cdots + a_1 s + a_0 = 0 \quad (11)$$

Then, the necessary condition for the stability of linear systems is that the coefficients of characteristic polynomials are positive, that is, the coefficients of characteristic polynomials are positive as follows [42]:

$$a_n > 0, a_{n-1} > 0, \ldots, a_0 > 0 \quad (12)$$

With theorem 2, we can analyze the open-loop stability of the maglev system. For the transfer function (10) of the magnetic suspension system, it is obvious that $a_0 = -R_m P_x < 0$ in the characteristic polynomial. So the system is unstable by theorem 2.

Remark 4: The open-loop of maglev system is unstable. It is necessary to design a feedback controller for active regulation to ensure vertical security.

Remark 5: The original mathematical model of magnetic suspension system (1) is strongly non-linear and beyond the scope of application of traditional linear control strategy.

III. Design of Extended State Observer (ESO)

In the actual maglev train suspension system, the chopper is used to supply the suspension electromagnet, and the current following principle is utilized to adjust the current of the electromagnet. Therefore, the current loop is used to control when designing the controller.

For maglev train system, it can be transformed into the following state space equation as follows:

$$\begin{cases} \dot{x}_1 = x_2 \\ \dot{x}_2 = g - bu + f(t) \end{cases} \quad (13)$$

where $b = \frac{\kappa}{mx_1^2}$, $u = i^2$, $f(t) = \frac{\delta(t)}{m}$. x_1 denotes airgap; x_2 is airgap velocity, u represents control input; g denotes gravity acceleration.

The expanded state observer is used to obtain airgap velocity and external disturbance of maglev train. The expanded state observer is designed as follows:

$$\begin{cases} \dot{\hat{x}}_1 = \hat{x}_2 + \eta_1(x_1 - \hat{x}_1) \\ \dot{\hat{x}}_2 = g - bu + \hat{x}_3 + \eta_2(x_1 - \hat{x}_1) \\ \dot{\hat{x}}_3 = \eta_3(x_1 - \hat{x}_1) \end{cases} \quad (14)$$

where $\eta_1 = \frac{\alpha_1}{\varepsilon}, \eta_2 = \frac{\alpha_2}{\varepsilon^2}, \eta_3 = \frac{\alpha_3}{\varepsilon^3}$, $\varepsilon > 0, \alpha_1, \alpha_2, \alpha_3$ are positive real numbers; $\hat{x}_1$ denotes the estimate value of x_1; $\hat{x}_2$ is the estimate value of x_2; $\hat{x}_3$ is the estimate of disturbance $f(t)$; $\left|\dot{f}\right| \leq L$. The observation error should be analyzed mathematically.

To this end, let

$$\gamma = \begin{bmatrix} \gamma_1 & \gamma_2 & \gamma_3 \end{bmatrix}^T$$

where

$$\gamma_1 = \frac{\tilde{x}_1}{\varepsilon^2}, \quad \gamma_2 = \frac{\tilde{x}_2}{\varepsilon}, \quad \gamma_3 = \tilde{x}_3, \quad \tilde{x}_1 = x_1 - \hat{x}_1, \quad \tilde{x}_2 = x_2 - \hat{x}_2, \quad \tilde{x}_3 = x_3 - \hat{x}_3$$

Since:

$$\begin{cases} \varepsilon\dot{\gamma}_1 = -\alpha_1\gamma_1 + \gamma_2 \\ \varepsilon\dot{\gamma}_2 = -\alpha_2\gamma_1 + \gamma_3 \\ \varepsilon\dot{\gamma}_3 = -\alpha_3\gamma_1 + \varepsilon\dot{f}(t) \end{cases} \quad (15)$$

The equation of state of observation error can be written as follows:

$$\varepsilon\dot{\gamma} = \mathrm{A}\gamma + \varepsilon\mathrm{B}\dot{f} \quad (16)$$

where $\mathrm{A} = \begin{bmatrix} -\alpha_1 & 1 & 0 \\ -\alpha_2 & 0 & 1 \\ -\alpha_3 & 0 & 0 \end{bmatrix}, \mathrm{B} = \begin{bmatrix} 0 \\ 0 \\ 1 \end{bmatrix}$. The characteristic equation of matrix A is described as follows:

$$\lambda^3 + \alpha_1\lambda^2 + \alpha_2\lambda + \alpha_3 = 0 \quad (17)$$

By selecting $\alpha_i (i = 1, 2, 3)$, A is obtained to satisfy the Hurwitz criterion [43].

Then for any given symmetric positive definite matrix Q, there exists a symmetric positive definite matrix P satisfying the following Lyapunov equation:

$$\mathrm{A}^{\mathrm{T}}\mathrm{P} + \mathrm{PA} + \mathrm{Q} = 0 \quad (18)$$

The Lyapunov function of the observer is defined as follows:

$$V_0 = \varepsilon\gamma^{\mathrm{T}}\mathrm{P}\gamma \quad (19)$$

Therefore:

$$\begin{aligned} \dot{V}_0 &= \varepsilon\dot{\gamma}^{\mathrm{T}}\mathrm{P}\gamma + \varepsilon\gamma^{\mathrm{T}}\mathrm{P}\dot{\gamma} = (\mathrm{A}\gamma + \varepsilon\mathrm{B}\dot{f})^T\mathrm{P}\gamma \\ &\quad + \gamma^T\mathrm{P}(\mathrm{A}\gamma + \varepsilon\mathrm{B}\dot{f}) = \gamma^{\mathrm{T}}(\mathrm{A}^T\mathrm{P} + \mathrm{PA})\gamma \\ &\quad + 2\varepsilon\gamma^T\mathrm{PB}\dot{f} \leq -\gamma^T\mathrm{Q}\gamma + 2\varepsilon\|\mathrm{PB}\| \cdot \|\gamma\| \cdot \left|\dot{f}\right| \\ &\leq -\lambda_{\min}(\mathrm{Q})\|\gamma\|^2 + 2\varepsilon L\|\mathrm{PB}\| \cdot \|\gamma\| \end{aligned} \quad (20)$$

where $\lambda_{\min}(\mathrm{Q})$ denotes the minimum eigenvalue of Q.

The convergence condition of observer obtained from $\dot{V}_0 \leq 0$ is:

$$\|\gamma\| \leq \frac{2\varepsilon L\|\mathrm{PB}\|}{\lambda_{\min}(\mathrm{Q})} \quad (21)$$

(21) shows that the convergence rate of observation error γ is related to ε. The smaller ε is, the faster γ converges. With the decrease of ε, the observation error tends to zero.

IV. Semi-Supervised Control Design Based on Deep Belief Network Algorithm

A. Output-Constrained Controller Design

On the basis of the proposed extended state observer, the airgap of the system output x_1 is limited within physical permissible range, and the controller is designed by using

the backstepping method to ensure its stability. By introducing inter virtual control variable, the backstepping method decomposes the complex nonlinear system into subsystems that do not exceed the order of the system. Then the Lyapunov functions of each subsystem are designed in sequence to develop the whole control law.

The airgap error e_1 is defined as follows:

$$e_1 = x_1 - x_{1d} \tag{22}$$

where x_1 denotes airgap of the system output; x_{1d} is the reference airgap. The limitation range of x_1 is $(x_{\min}, x_{\max})$.

The inter virtual control variable β of the backstepping control is defined as follows:

$$\beta = -k_1 e_1 - \frac{e_1}{k_b^2 - e_1^2} \tag{23}$$

where $k_1 \in R^+$ denotes the control gain.

Simultaneously, e_2 can be designed as below:

$$e_2 = \hat{x}_2 - \beta - \dot{x}_{1d} \tag{24}$$

Based on (22) and (24), we can obtain the following equation:

$$\dot{e}_1 = e_2 + \beta + \tilde{x}_2 \tag{25}$$

If $|e_1| < k_b$, then we can get:

$$-k_b + x_{1d\min} < x_1 < k_b + x_{1d\max} \tag{26}$$

Therefore, x_1 can be guaranteed in the limitation range by setting the value of k_b. The proposed controller can be represented in the following fashion:

$$u = \frac{1}{b}(\hat{x}_3 + \eta_2(x_1 - \hat{x}_1) - \dot{\beta} - \ddot{x}_{1d} + k_2 e_2 + g + \frac{e_1}{k_b^2 - e_1^2}) \tag{27}$$

where $k_2 \in R^+$ represents the control parameter.

B. Closed-Loop Stability Analysis

The stability of general extended state observer (ESO) and proposed control method has been proved separately. In this section, the entire stability of the presented intelligent control fused with the developed ESO is proved.

A symmetric Barrier Lyapunov function is defined as follows:

$$V_1 = \varepsilon \gamma^T \mathrm{p} \gamma + \frac{1}{2} \log \frac{k_b^2}{k_b^2 - e_1^2} \tag{28}$$

By taking the time derivative of $V_1(t)$ in (28), substituting (20) and (25) into the resulting equation, canceling out the common terms, and making some arrangements, we can get the following results:

$$\dot{V}_1 \le -\lambda_{\min}(\mathrm{Q}) \|\gamma\|^2 + 2\varepsilon L \|\mathrm{PB}\| \cdot \|\gamma\| + \frac{e_1(e_1 + \beta + \tilde{x}_2)}{k_b^2 - e_1^2} \tag{29}$$

By using Young's inequality, the second and third terms in (29) can be arranged as follows:

$$2\varepsilon L \|\mathrm{PB}\| \cdot \|\gamma\| \le \varepsilon L(\|\mathrm{PB}\|^2 + \|\gamma\|^2) \tag{30}$$

$$\begin{aligned} \frac{e_1 \tilde{x}_2}{k_b^2 - e_1^2} &\le \frac{1}{2}[\frac{e_1^2}{(k_b^2 - e_1^2)^2} + |\tilde{x}_2|^2] \\ &\le \frac{e_1^2}{(k_b^2 - e_1^2)^2} + \frac{|\varepsilon \gamma_2|^2}{2} \end{aligned} \tag{31}$$

By inserting (30) and (31) into (29), and arranging the obtained results, one can reorganize (29) as follows:

$$\begin{aligned} \dot{V}_1 &\le -\lambda_{\min}(\mathrm{Q}) \|\gamma\|^2 + \varepsilon L \|\gamma\|^2 + \varepsilon L \|\mathrm{PB}\|^2 \\ &\quad + \frac{\varepsilon^2}{2} |\gamma_2|^2 + \frac{e_1^2}{(k_b^2 - e_1^2)^2} + \frac{e_1(e_2 + \beta)}{k_b^2 - e_1^2} \\ &= -[\lambda_{\min}(\mathrm{Q}) - \varepsilon L)] \|\gamma\|^2 + \rho \\ &\quad - \frac{k_1 e_1^2}{k_b^2 - e_1^2} + \frac{e_1 e_2}{k_b^2 - e_1^2} \end{aligned} \tag{32}$$

where $\rho = \varepsilon L \|\mathrm{PB}\|^2 + \frac{\varepsilon^2}{2} |\gamma_2|^2$.

Since x_2 does not need to be restricted and the proposed control law (27) is introduced, the Lyapunov candidate function can be defined as follows:

$$V = V_1 + \frac{1}{2} e_2^2 \tag{33}$$

By taking the time derivative of $V(t)$ in (33), and arranging the obtained results, we can get the following result:

$$\begin{aligned} \dot{V} &= \dot{V}_1 + e_2 \dot{e}_2 \le -[\lambda_{\min}(\mathrm{Q}) - \varepsilon L] \|\gamma\|^2 \\ &\quad + \rho - \frac{k_1 e_1^2}{k_b^2 - e_1^2} + \frac{e_1 e_2}{k_b^2 - e_1^2} + e_2(\dot{\hat{x}}_2 - \dot{\beta} - \ddot{x}_{1d}) \\ &= -[\lambda_{\min}(\mathrm{Q}) - \varepsilon L] \|\gamma\|^2 + \rho - \frac{k_1 e_1^2}{k_b^2 - e_1^2} \\ &\quad + e_2(\dot{\hat{x}}_2 - \dot{\beta} - \ddot{x}_{1d} + \frac{e_1}{k_b^2 - e_1^2}) \\ &= -[\lambda_{\min}(\mathrm{Q}) - \varepsilon L] \|\gamma\|^2 + \rho - \frac{k_1 e_1^2}{k_b^2 - e_1^2} \\ &\quad + e_2[g - bu + \hat{x}_3 + \eta_2(x_1 - \hat{x}_1) - \dot{\beta} - \ddot{x}_{1d} + \frac{e_1}{k_b^2 - e_1^2}] \\ &\quad - [\lambda_{\min}(\mathrm{Q}) - \varepsilon L] \|\gamma\|^2 + \rho - \frac{k_1 e_1^2}{k_b^2 - e_1^2} - k_2 e_2^2 \end{aligned} \tag{34}$$

The following inequality (35) holds [44]:

$$-\frac{k_1 e_1^2}{k_b^2 - e_1^2} \le -\log \frac{k_b^2}{k_b^2 - e_1^2} \tag{35}$$

Using the fact of (35), the (34) can be processed as:

$$\begin{aligned} \dot{V} &\le -[\lambda_{\min}(\mathrm{Q}) - \varepsilon L)] \|\gamma\|^2 + \rho \\ &\quad - \log \frac{k_b^2}{k_b^2 - e_1^2} - k_2 e_2^2 \le -cV + \lambda \end{aligned} \tag{36}$$

where $c = \min\{\frac{\lambda_{\min}(\mathrm{Q}) - \varepsilon L}{\lambda_{\min}(\mathrm{p})}, 2, 2k_2\}$, $\lambda = \rho$.

The solution of inequality (36) is obtained as follows:

$$0 \le V \le V(t_0) e^{-c(t - t_0)} + \frac{\lambda}{c} \tag{37}$$

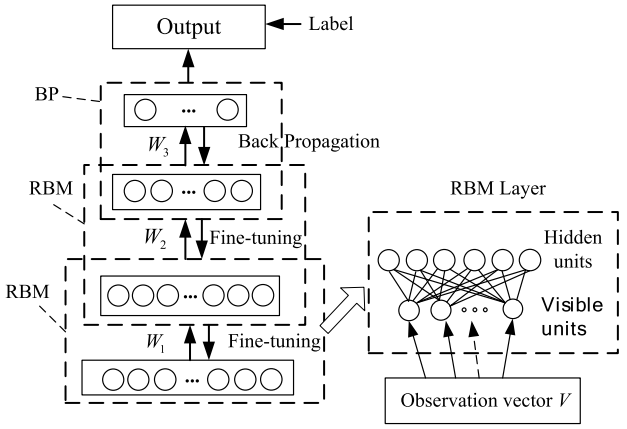

Fig. 2. Structure of deep belief network (DBN).

It is indicated from (37) that

$$\lim_{t\to\infty} V = \frac{\lambda}{c} \tag{38}$$

(37) and (38) demonstrate that $V(t)$ is within the sphere with the origin as the center of the sphere and the radius of $\frac{\lambda}{c}$, that is $V(t)$ uniformly ultimately bounded. It is shown that this method can stabilize the system and restrict the airgap in the limited range.

C. DBN Semi-Supervised Control

The deep belief network is trained by stacking multiple layers of restricted Boltzmann machine (RBM), and a supervised reverse iterative layer is added to the last layer to achieve the overall fine-tuning, as shown in Fig. 2.

RBM is a typical undirected graph model in which the visible layer υ is connected to the hidden layer h through an undirected weighted connection [46], [47]. RBM can be defined as a probability distribution model through an energy function. Assuming it is a binary RBM, you can obtain:

$$\begin{aligned} -\log p(\upsilon, h) &\propto E(\upsilon, h; \theta) \\ &= -\sum_{i=1}^{|V|}\sum_{j=1}^{|H|} w_{ij}\upsilon_i h_j - \sum_{i=1}^{|V|} b_i\upsilon_i - \sum_{j=1}^{|H|} a_j h_j \end{aligned} \tag{39}$$

where $\theta = (w, a, b)$ is the parameter set, w_{ij} is the symmetrical weight between the visible unit i and the hidden unit j; a_j is the offset of the visible layer, and b_i is the offset of the hidden layer. The number of visible units and hidden units can be expressed as $|V|$ and $|H|$, respectively. When υ and h do not changes, the structures make it easier to calculate the conditional probability distribution, as follows:

$$p(h_j\,|\upsilon\,;\theta) = sigm(\sum_{i=1}^{|V|} w_{ij}\upsilon_i + a_j) \tag{40}$$

$$p(\upsilon_i\,|h\,;\theta) = sigm(\sum_{j=1}^{|H|} w_{ij}h_j + b_i) \tag{41}$$

where $\mathrm{sigm}(x) = (1/(1+e^{-x}))$ is a sigmoid function. The model parameters $\theta = (w, a, b)$ can be learned by the contrast divergence algorithm (CD-k) [35].

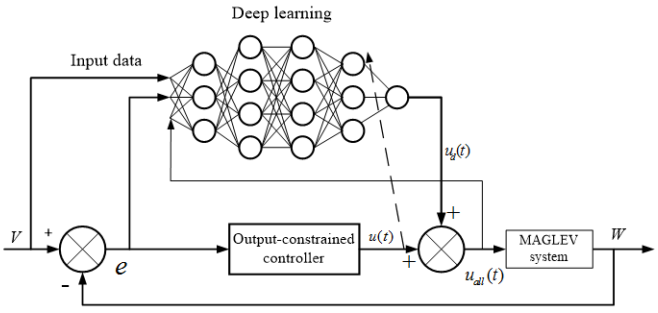

Fig. 3. Structure of Semi-Supervised Controller based on DBN.

The DBN network training process canbe divided into two stages: pre-training and fine tuning. In the stage of pre-training, each layer of RBM network is independently and unsupervised trained to ensure that as much feature information is retained as possible when the feature vectors are mapped to different feature spaces. In the stage of fine tuning, the weights between the trained RBMs are utilized as the initial weights of the DBN. Additionally, the network labels are utilized as the supervised signals to calculate the network error. The Back Propagation (BP) algorithm is utilized to calculate the error of each layer to adjust the weights of each layer based on the gradient descent method.

As shown in Fig 3, the DBN semi-supervised control (DBN SSC) is expected to gradually replace the output-constrained controller u with the deep learning output control input u_d, after online learning in the control process.

The neural network-based supervisor controller (NNBSC) $u_{all}(t)$ is designed as follows:

$$u_{all}(t) = u(t) + u_d(t) \tag{42}$$

The weights can the be adjusted according to the stochastic gradient descent method [35].

V. Simulation Results

In order to verify that the above theory can accurately estimate various states and external disturbances, and at the same time can restrict the output within a limited range, this section will carry out numerical simulation analysis. Considering the actual situation, the limited range of airgap x_1 is $(0, 0.016)$; initial position $x_1(t_0) = 0.016m$; reference airgap $x_{1d} = 0.008m$; force transmission coefficient $\kappa = 0.00076$; mass $m = 750kg$; gravity acceleration $g = 9.8m/s^2$; ESO parameters are chosen as: $\alpha_1 = 6$, $\alpha_2 = 11$, $\alpha_3 = 6$, $\varepsilon = 0.01$; backstepping control parameters are selected as: $k_1 = 3$, $k_2 = 10$; RBM hidden layer consists of three layers, each layer contains 650 neurons, the learning rate is 0.2, the iteration number is 500, and the dropout rate is 0.3; the external disturbance force is chosen as:

$$f(t) = 36000\sin(2t + \pi/2) - 40000\sin(4t + \pi/2) \tag{43}$$

Based on the limited range of x_1 and (26), we can obtained that $k_b = 0.008$.

In order to further illustrate the superiority of the proposed DBN semi-supervised control method, the dynamic response

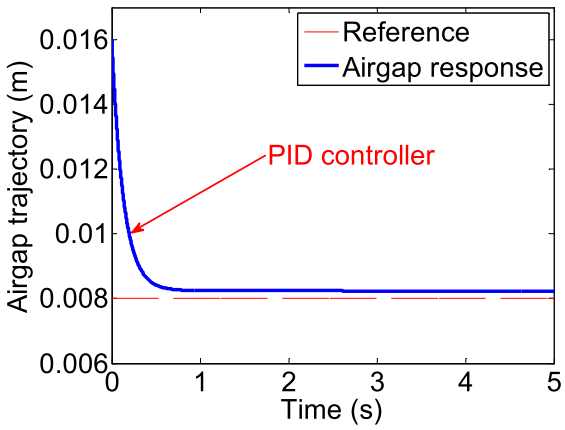

Fig. 4. Airgap response with PID.

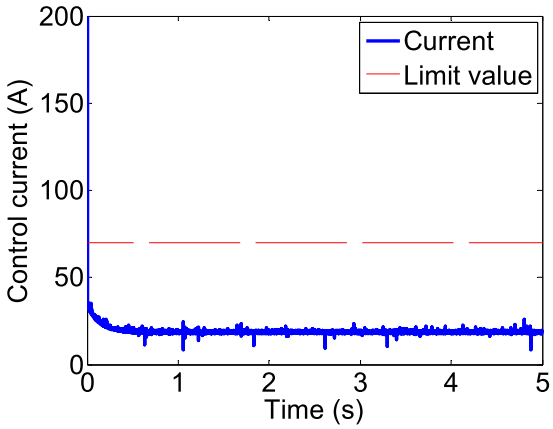

Fig. 5. Control input with PID.

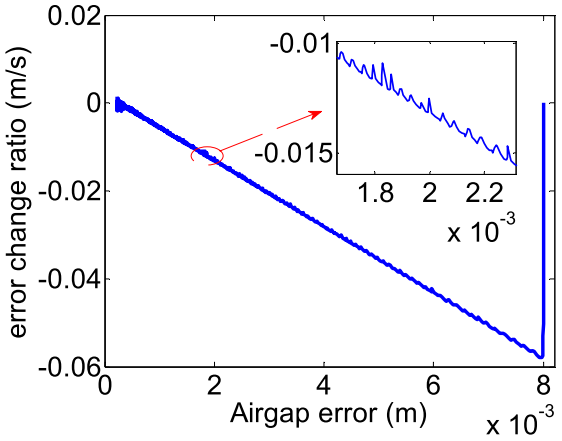

Fig. 6. Phase locus with PID.

of the system is also simulated under the action of the proportion-integral-differential (PID) controller with the same working condition. The trial-and-error method is utilized to determine the best control parameters of PID, which are: $P = 56000$, $I = 500$, $D = 7400$.

In the static suspension case without disturbance, the simulation results of the PID controller are shown in Figs. 4-6.

The external disturbance $f(t)$ in (43) is applied to the nonlinear system. The airgap response is illustrated in Fig. 7.

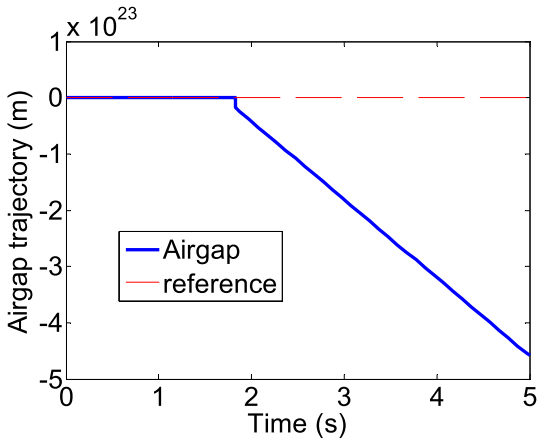

Fig. 7. Airgap response with PID under disturbance.

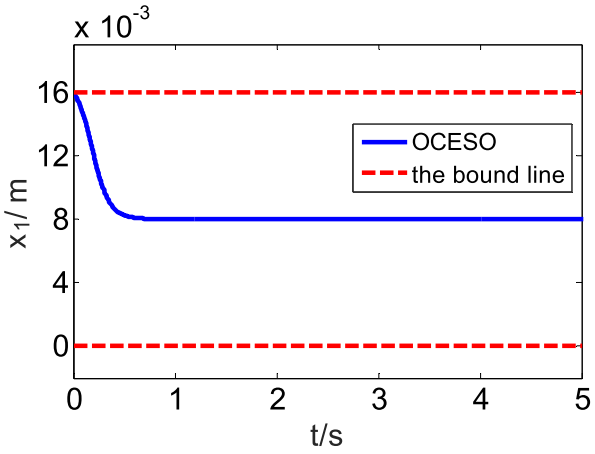

Fig. 8. Airgap and its bounded range with disturbance.

We can learn from the Figs. 4-6 that under the action of the PID controller, there is a static error in the airgap response, and the maximum steady state error is 0.25 mm. The maximum control circuit reaches 200A, which far exceed the current limit of 70A at the beginning. There are some fluctuations in control current signals, which are caused by the excessive gain. But, a small gain will lead to the system to be unstable, which will affect the vertical security. This discussion also can be proved in Fig. 7 when we applied the disturbance to the system. We can see from Fig. 7 that when the nonlinear periodic disturbance is applied to system, the PID controller cannot stabilize the system and the system becomes instability.

When the proposed deep learning controller is applied to the system, the simulation results of airgap with disturbance and its bounded airgap range are shown in Fig. 8.

The simulation results of airgap error are shown in Fig. 9.

The airgap velocity x_2 and the estimate value $\hat{x}_2$ obtained by proposed ESO are included in Fig. 10.

The external disturbance $f(t)$ and the estimate value $\hat{x}_3$ obtained by proposed ESO are shown in Fig. 11.

Figs. 8-9 show that the proposed semi-supervised control based on deep belief network can constrain the air gap between the bounded airgap, and the airgap can converge quickly to the target position within about 0.5 seconds smoothly. Fig. 10 shows the airgap velocity and its estimation results.

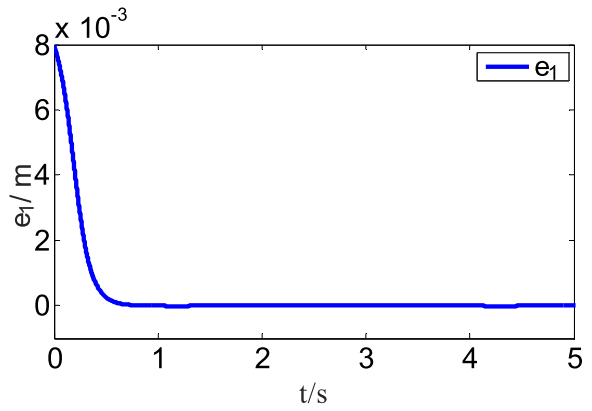

Fig. 9. Simulation results of airgap error with disturbance.

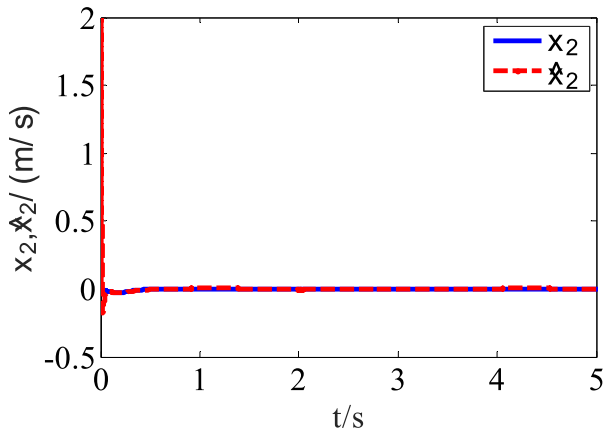

Fig. 10. Simulation results of airgap velocity and estimate value.

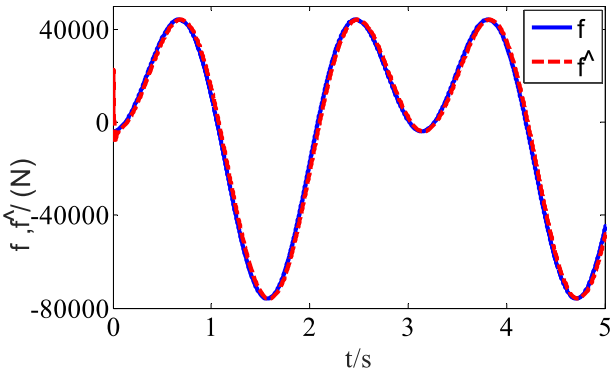

Fig. 11. Simulation results of disturbances and its estimation.

In less than 0.1 seconds, the estimate value $\hat{x}_2$ coincides with the airgap velocity x_2. It can be seen that the proposed ESO can estimate the airgap velocity quickly and accurately. Fig. 11 shows the disturbance and its estimation value. It can be learned that the observer can estimate the disturbance accurately and quickly, which guarantees the stability and control accuracy of the system. In summary, the propose control strategy can estimate the airgap velocity and unknown external interference effectively and rapidly, while ensuring the stable suspension within the bounded airgap range during the whole suspension process.

TABLE I

SIMULATION RESULTS COMPARISON WITH EXTERNAL DISTURBANCE

Method	Steady state error	Max error	Chattering	Within limitations
PID	Unstable	/	Bit	No
SMC	-1.2 mm	1.7 mm	Yes	Yes
MFC	Unstable	/	None	No
OCC	-0.23 mm	0.31 mm	None	Yes
DBN-SSC	-0.21mm	0.3 mm	none	Yes

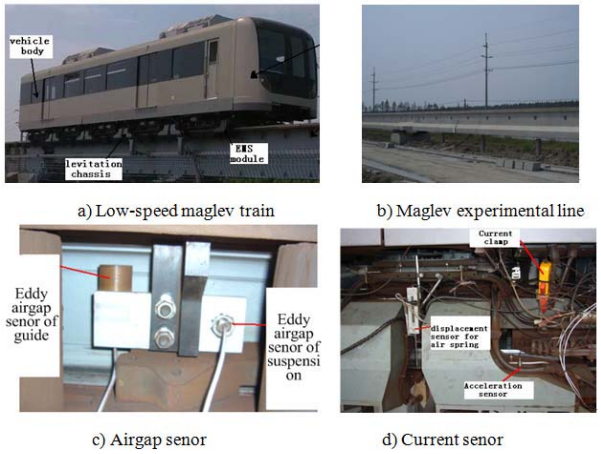

Fig. 12. Full-scale experimental maglev vehicle system.

In order to show superiority of the proposed DBN semi-supervised control (DBN-SSC), the performance of DBN-SSC is validated in simulation with compared with the PID [45], output-constrained controller (OCC), sliding mode controller (SMC) [45] and modified fuzzy controller[2]. The simulation results of applying external disturbance in (43) are listed in Table I.

VI. EXPERIMENTAL IMPLEMENTATION AND RESULTS

After sufficient simulation tests, much effort have been put to perform experiments with the aim of examining the practical performance of the proposed deep belief network based semi-supervised controller. The experiments are implemented on a full-scale maglev system testbed [23], whose core parts are illustrated in Fig. 12. The maglev control system includes eddy airgap sensor, A/D acquisition card, acceleration sensor and chopper. The maglev test line is about 1.7 km. The track irregularity disturbance is made in advance on the test line track. The USB-CAN is utilized to design a debugging system and PC human-machine interface is written in C#.

The sampling frequency of the testbed is 1000 Hz. The target airgap of the full-scale maglev vehicle during operation is 8mm, and the initial airgap is 16mm. So, the bounded airgap range is $\left(0,\ 16mm\right)$ and the values of test parameters of proposed deep learning controller are the same as the values in the simulation section. Experiments are implemented to investigate and verify the disturbance rejection capacity of the presented deep learning semi-supervised control method compared with the widely used PID controller. Two sets of

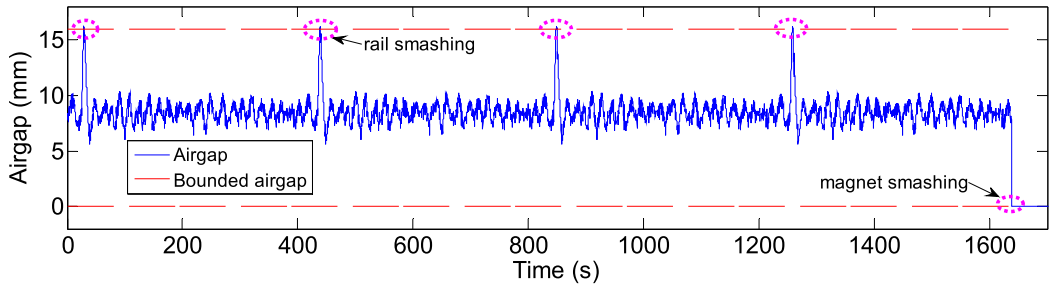

Fig. 13. Airgap response with PID controller.

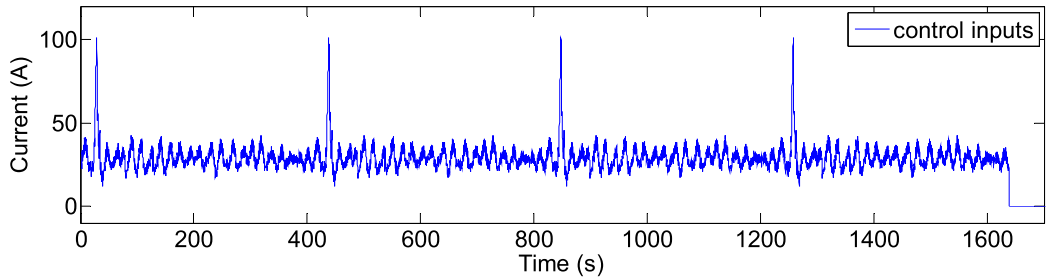

Fig. 14. Current response with PID controller.

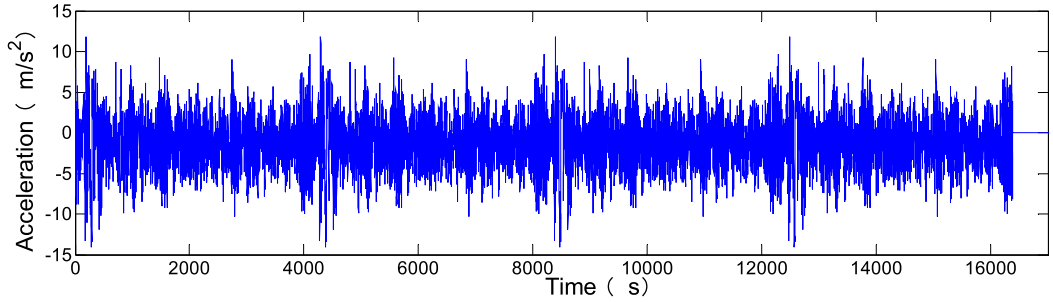

Fig. 15. Acceleration response of electromagnet with PID controller.

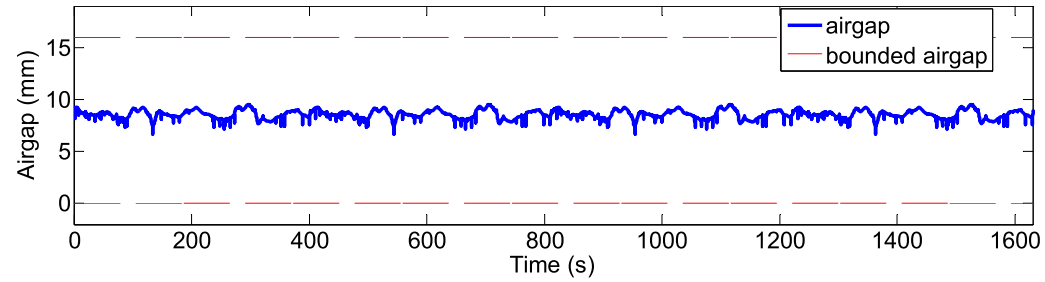

Fig. 16. Airgap response with deep learning semi-supervised controller.

experiments are performed to verify the vertical security and the control performance.

Experiment 1: The maglev vehicle is running under the track irregularity disturbance with the PID controller. The experimental results of Experiment 1 are provided in Figs. 13-15.

Experiment 2: The maglev vehicle is running under the track irregularity disturbance with the proposed deep learning semi-supervised controller. The experimental results of Experiment 2 are recorded in Figs. 16-18.

By summarizing the foregoing two experiments 1-2, it is concluded that the proposed deep learning semi-supervised control strategy can achieve better control performance over PID controller with track irregularity disturbance. In particular, by comparing Figs. 13 and 15, we see that the airgap of the system with PID reaches 16mm, which means the maglev vehicle collides with the track (called "rail smashing"). But the airgap of proposed semi-supervised controller is within 6∼9mm without "rail smashing" and "magnet smashing", which is more stable than that of the PID method.

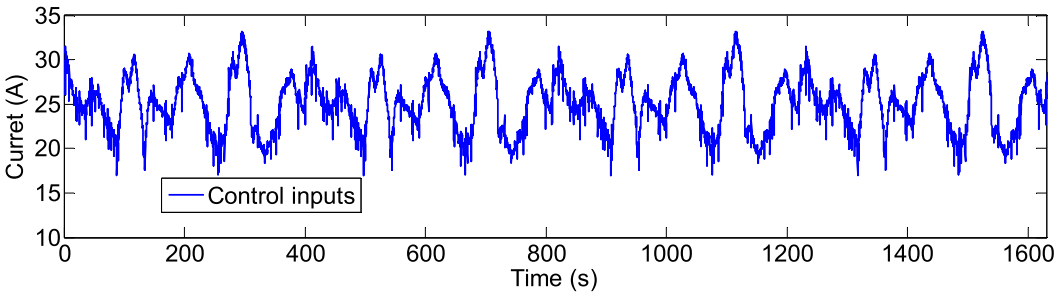

Fig. 17. Current response with deep learning semi-supervised controller.

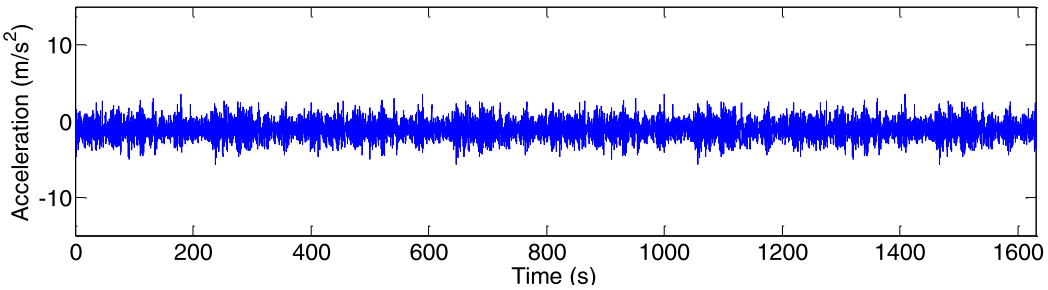

Fig. 18. Acceleration response of electromagnet with semi-supervised controller.

TABLE II
EXPERIMENTAL RESULTS COMPARISON

Method	Max airgap	Max current	Max acceleration	Within Bounded Airgap
PID	16 mm	100 A	14 m/s^2	No
DBN SSC	9.6 mm	33 A	6.2 m/s^2	Yes

Moreover, the control inputs of PID and deep learning semi-supervised controller are compared in Figs. 14 and 17. We can learn that the control input of deep learning semi-supervised controller is smaller than PID controller mainly due to feedforward compensation by the ESO. The acceleration response of electromagnet with PID controller is greater than that of the deep learning semi-supervised control method, which means deep learning semi-supervised can provide more ride comfort for passengers. These experiment results demonstrate satisfactory robustness of the presented control strategy based on deep learning, which can guarantee the airgap state within the bounded airgap range. The experimental results analysis of different controllers is shown in Table II.

Thus, we can conclude that the proposed deep learning based semi-supervised control is more effective to guarantee the bounded airgap in actual operation of the maglev train.

VII. CONCLUSION

Aiming at the problem of the vertical security with external disturbance, unmeasurable airgap velocity and limited airgap rang, this paper develops an expanded state observer (ESO) to estimate the airgap velocity $x_2(t)$ and generalized disturbance $f(t)$ online, which can be utilized as feedforward compensation of the controller for the maglev system. The output-constraints and ESO estimates are fused to design the control law based on backstepping control method, and then stability analysis is carried out based on symmetric Barrier Lyapunov function. The deep belief network is utilized to combine with output-constraints controller to develop a deep learning semi-supervised control strategy. According to the actual situation of the magnetic suspension system of maglev vehicle, the simulation with specify parameters and experiment are carried out respectively to examining the practical performance of the proposed deep learning semi-supervised controller. The simulation and experimental results demonstrate that the proposed control method can effectively deal with the unmeasurable airgap velocity and unknown generalized disturbance simultaneously. The proposed controller has strong robustness and ensures that the output airgap is within the physical limit all the time, which can solve the problem of maglev train crashing to rail in the train operation.

REFERENCES

[1] H.-W. Lee, K.-C. Kim, and J. Lee, "Review of maglev train technologies," *IEEE Trans. Magn.*, vol. 42, no. 7, pp. 1917–1925, Jul. 2006.
[2] Y. Sun, H. Qiang, J. Xu, and G. Lin, "Internet of Things-based online condition monitor and improved adaptive fuzzy control for a Medium-Low-Speed maglev train system," *IEEE Trans. Ind. Informat.*, vol. 16, no. 4, pp. 2629–2639, Apr. 2020.
[3] I. Boldea, L. N. Tutelea, W. Xu, and M. Pucci, "Linear electric machines, drives, and MAGLEVs: An overview," *IEEE Trans. Ind. Electron.*, vol. 65, no. 9, pp. 7504–7515, Sep. 2018.
[4] C. Chen, J. Xu, G. Lin, Y. Sun, and D. Gao, "Fuzzy adaptive control particle swarm optimization based on T-S fuzzy model of maglev vehicle suspension system," *J. Mech. Sci. Technol.*, vol. 34, no. 1, pp. 43–54, Jan. 2020.
[5] X. Zhang, M. Mehrtash, and M. B. Khamesee, "Dual-axial motion control of a magnetic levitation system using Hall-effect sensors," *IEEE/ASME Trans. Mechatronics*, vol. 21, no. 2, pp. 1129–1139, Apr. 2016.

[6] Y. Sun, J. Xu, H. Qiang, C. Chen, and G. Lin, "Adaptive sliding mode control of maglev system based on RBF neural network minimum parameter learning method," *Measurement*, vol. 141, pp. 217–226, Jul. 2019.

[7] S. Dai *et al.*, "Estimation of speed and acceleration of the maglev platform by state observer," *J. Shandong Univ.*, vol. 48, no. 2, pp. 114–120, 2018.

[8] X. Bu, "Air-breathing hypersonic vehicles funnel control using neural approximation of non-affine dynamics," *IEEE/ASME Trans. Mechatronics*, vol. 23, no. 5, pp. 2099–2108, Oct. 2018.

[9] X. Bu, X. Wu, R. Zhang, Z. Ma, and J. Huang, "A neural approximation-based novel back-stepping control scheme for air-breathing hypersonic vehicles with uncertain parameters," *Proc. Inst. Mech. Eng., I, J. Syst. Control Eng.*, vol. 230, no. 3, pp. 231–243, Mar. 2016.

[10] X. Bu, G. He, and K. Wang, "Tracking control of air-breathing hypersonic vehicles with non-affine dynamics via improved neural back-stepping design," *ISA Trans.*, vol. 75, pp. 88–100, Apr. 2018.

[11] R. Michino, H. Tanaka, and I. Mizumoto, "Application of high gain adaptive output feedback control to a magnetic levitation system," in *Proc. ICCAS-SICE*, Dec. 2009, pp. 970–975.

[12] B. Liu and W. Zhou, "Backstepping based nonlinear adaptive control of magnetic levitation system with unknown disturbances," in *Proc. 5th Int. Conf. Intell. Human-Machine Syst. Cybern.*, Aug. 2013, pp. 11–14.

[13] W. Saikia and A. Saikia, "Magnetic levitation system control strategy based on backstepping technique to design sliding mode controller," in *Proc. 2nd Int. Conf. Power, Energy Environ., Towards Smart Technol. (ICEPE)*, Jun. 2018, pp. 1–4.

[14] W. Chen, J. Yang, L. Guo, and S. Li, "Disturbance-observer-based control and related methods-an overview," *IEEE Trans. Ind. Electron.*, vol. 63, no. 2, pp. 1083–1095, Feb. 2016.

[15] J. Yang, T. Li, C. Liu, S. Li, and W.-H. Chen, "Nonlinearity estimator-based control of a class of uncertain nonlinear systems," *IEEE Trans. Autom. Control*, vol. 65, no. 5, pp. 2230–2236, May 2020.

[16] S. Ding, W.-H. Chen, K. Mei, and D. J. Murray-Smith, "Disturbance observer design for nonlinear systems represented by input–output models," *IEEE Trans. Ind. Electron.*, vol. 67, no. 2, pp. 1222–1232, Feb. 2020.

[17] B. Liu and W. Tang, *Modern Control Theory*, Beijing: China: Machine Press, 2006.

[18] J. Han, "From PID to active disturbance rejection control," *IEEE Trans. Ind. Electron.*, vol. 56, no. 3, pp. 900–906, Dec. 2009.

[19] B. Du, S. Wu, S. Han, and S. Cui, "Application of linear active disturbance rejection controller for sensorless control of internal permanent-magnet synchronous motor," *IEEE Trans. Ind. Electron.*, vol. 63, no. 5, pp. 3019–3027, Jan. 2016.

[20] B.-Z. Guo and Z.-L. Zhao, "On the convergence of an extended state observer for nonlinear systems with uncertainty," *Syst. Control Lett.*, vol. 60, no. 6, pp. 420–430, Jun. 2011.

[21] P. He and X. Wang, "The research of the novel bearingless levitation system based on extended state observer (ESO)," in *Proc. Int. Conf. Electr. Mach. Syst.*, Aug. 2011, pp. 1–6.

[22] L. Zhao, X. Liu, and T. Wang, "Trajectory tracking control for double-joint manipulator systems driven by pneumatic artificial muscles based on a nonlinear extended state observer," *Mech. Syst. Signal Process.*, vol. 122, pp. 307–320, May 2019.

[23] Y. Sun, J. Xu, H. Qiang, and G. Lin, "Adaptive neural-fuzzy robust position control scheme for maglev train systems with experimental verification," *IEEE Trans. Ind. Electron.*, vol. 66, no. 11, pp. 8589–8599, Nov. 2019.

[24] R.-J. Wai, M.-W. Chen, and J.-X. Yao, "Observer-based adaptive fuzzy-neural-network control for hybrid maglev transportation system," *Neurocomputing*, vol. 175, pp. 10–24, Jan. 2016.

[25] S. Chen *et al.*, "Vibration state estimation of nonlinear suspension system based on feedback linearization," *J. Vib. Shock*, vol. 34, no. 20, pp. 10–15, 2018.

[26] H. Wang, X. Ge, and Y.-C. Liu, "Second-order sliding-mode MRAS observer-based sensorless vector control of linear induction motor drives for medium-low speed maglev applications," *IEEE Trans. Ind. Electron.*, vol. 65, no. 12, pp. 9938–9952, Dec. 2018.

[27] J. Xu, Y. Sun, D. Gao, W. Ma, S. Luo, and Q. Qian, "Dynamic modeling and adaptive sliding mode control for a maglev train system based on a magnetic flux observer," *IEEE Access*, vol. 6, pp. 31571–31579, 2018.

[28] Y. Sun, H. Qiang, X. Mei, and Y. Teng, "Modified repetitive learning control with unidirectional control input for uncertain nonlinear systems," *Neural Comput. Appl.*, vol. 30, no. 6, pp. 2003–2012, Sep. 2018.

[29] X. JIN and X. XU, "Iterative learning control for output-constrained systems with both parametric and nonparametric uncertainties," *Automatica*, vol. 49, no. 8, pp. 2508–2516, 2013.

[30] K. P. Tee, S. S. Ge, and E. H. Tay, "Barrier Lyapunov functions for the control of output-constrained nonlinear systems," *Automatica*, vol. 45, no. 4, pp. 918–927, Apr. 2009.

[31] B. Singh and V. Kumar, "A real time application of model reference adaptive PID controller for magnetic levitation system," in *Proc. IEEE Power, Commun. Inf. Technol. Conf. (PCITC)*, Oct. 2015, pp. 583–588.

[32] Y. Sun, J. Xu, H. Qiang, W. Wang, and G. Lin, "Hopf bifurcation analysis of maglev vehicle-guideway interaction vibration system and stability control based on fuzzy adaptive theory," *Comput. Ind.*, vol. 108, pp. 197–209, May 2019.

[33] J. Xu, Y. Du, Y.-H. Chen, and H. Guo, "Adaptive robust constrained state control for non-linear maglev vehicle with guaranteed bounded airgap," *IET Control Theory Appl.*, vol. 12, no. 11, pp. 1573–1583, Jul. 2018.

[34] Y. Lv, Y. Duan, W. Kang, Z. Li, and F.-Y. Wang, "Traffic flow prediction with big data: A deep learning approach," *IEEE Trans. Intell. Transp. Syst.*, vol. 16, no. 2, pp. 865–873, Apr. 2015.

[35] W. Huang, G. Song, H. Hong, and K. Xie, "Deep architecture for traffic flow prediction: Deep belief networks with multitask learning," *IEEE Trans. Intell. Transp. Syst.*, vol. 15, no. 5, pp. 2191–2201, Oct. 2014.

[36] S. Guo, Y. Lin, S. Li, Z. Chen, and H. Wan, "Deep Spatial–Temporal 3D convolutional neural networks for traffic data forecasting," *IEEE Trans. Intell. Transp. Syst.*, vol. 20, no. 10, pp. 3913–3926, Oct. 2019.

[37] G. E. Hinton, "Reducing the dimensionality of data with neural networks," *Science*, vol. 313, no. 5786, pp. 504–507, Jul. 2006.

[38] Y. Bengio, P. Lamblin, D. Popovici, and H. Larochelle, "Greedy layer-wise training of deep networks," in *Proc. Adv. Neural Inf. Process. Syst.* Cambridge, MA: MIT Press, 2007, pp. 153–160.

[39] Y. Lecun, L. Bottou, Y. Bengio, and P. Haffner, "Gradient-based learning applied to document recognition," *Proc. IEEE*, vol. 86, no. 11, pp. 2278–2324, May 1998.

[40] R. J. Williams and D. Zipser, "A learning algorithm for continually running fully recurrent neural networks," *Neural Comput.*, vol. 1, no. 2, pp. 270–280, Jun. 1989.

[41] M. Zhien and Z. Yicang, *Qualitative and Stability Methods for Ordinary Differential Equations*. Beijing, China: Science Press, 2001.

[42] S. P. Bhattacharyya, A. Datta, and L. H. Keel, *Linear Control Theory: Structure, Robustness, and Optimization*. Boca Raton, FL, USA: CRC Press, 2018.

[43] J. Liu, *Sliding Mode Variable Structure Control MATLAB Simulation*. Beijing, China: Tsinghua Univ. Press, 2015.

[44] B. Ren, S. Sam Ge, K. Peng Tee, and T. Heng Lee, "Adaptive neural control for output feedback nonlinear systems using a barrier Lyapunov function," *IEEE Trans. Neural Netw.*, vol. 21, no. 8, pp. 1339–1345, Aug. 2010.

[45] Y. Sun *et al.*, "Dynamic modeling and nonlinear control research on magnetic suspension systems of low-speed maglev train," *Tongji Daxue Xuebao/J. Tongji Univ.*, vol. 45, no. 5, pp. 741–749, 2017.

[46] Haghighi, "Intelligent robust control for cyber-physical systems of rotary gantry type under denial of service attack," *J. Supercomput.*, vol. 76, no. 4, pp. 3063–3085, 2020.

[47] F. Farivar, M. S. Haghighi, A. Jolfaei, and M. Alazab, "Artificial intelligence for detection, estimation, and compensation of malicious attacks in nonlinear cyber-physical systems and industrial IoT," *IEEE Trans. Ind. Informat.*, vol. 16, no. 4, pp. 2716–2725, Apr. 2020.

Yougang Sun (Member, IEEE) received the B.S. degree in material formation and control engineering from Soochow University, China, in 2011, the M.S. degree (Hons.) in mechatronics engineering from Shanghai Maritime University, China, in 2013, and the Ph.D. degree in mechatronics engineering from Tongji University, Shanghai, China, in 2017.

From 2013 to 2018, he was a Mechatronics Engineer with Shanghai Maritime University. Since 2018, he has been a Post-Doctoral Fellow with the National Maglev Transportation Engineering R&D Center, Tongji University. His current research interests include maglev trains, offshore cranes, quay cranes, and nonlinear control with applications to mechatronic systems.

Junqi Xu received the B.S. degree in industrial automation from Lanzhou Jiaotong University, Lanzhou, China, in 2000, and the M.S. degree in power electronics and power transmission from Southwest Jiaotong University, Chengdu, China, in 2003, where he is currently pursuing the Ph.D. degree.

From 2003 to 2012, he was an Electrical and Control Engineer with the Shanghai Maglev Transportation Engineering R&D Center. He is currently working with the National Maglev Transportation Engineering R&D Center, Tongji University, Shanghai, China. His research interests include levitation control technology of maglev train and coupling vibration between maglev train and track.

Han Wu received the B.S. degree in naval architecture and ocean engineering from Tianjin University, China, in 2010, and the Ph.D. degree in engineering mechanics from the Institute of Mechanics, Chinese Academy of Sciences, China, in 2015.

Since 2015, he has been an Assistant Research Fellow with the Institute of Mechanics, Chinese Academy of Sciences. His current research interests include stability and response of high-speed railway train, and ocean structures, and also dynamics and control of maglev trains.

Guobin Lin received the B.S. degree in electric machine from Zhejiang University, Hangzhou, China, in 1986, and the M.S. degree in electrical engineering from Southwest Jiaotong University, China, in 1989.

He is currently a Professor and the Deputy Director of the National Maglev Transportation Engineering R&D Center, Tongji University. His research interests include maglev vehicle and linear drive research.

Dr. Lin has been a member of Steering Committee of International Maglev System and Linear Drive Conference since 2014.

Shahid Mumtaz (Senior Member, IEEE) received the master's degree in electrical and electronic engineering from the Blekinge Institute of Technology, Sweden, in 2006, and the Ph.D. degree in electrical and electronic engineering from the University of Aveiro, Portugal, in 2011.

He has more than 12 years of wireless industry/academic experience. He is the author of four technical books, 12 book chapters, over 180 technical papers (150+ journal/transaction and 80+ conferences), and received two IEEE Best Paper Award in the area of mobile communications. Most of his publications are in the field of cybersecurity and network security. He is serving as a scientific expert and an evaluator for various research funding agencies. He was awarded the "Alain Bensoussan Fellowship" in 2012. He was a recipient of the NSFC Researcher Fund for Young Scientist, China, in 2017. He is an ACM Distinguished Speaker, the Founder and EiC of *IET Quantum Communication*," the Vice-Chair of Europe/Africa Region-IEEE ComSoc: Green Communications & Computing society and of IEEE standard on P1932.1: Standard for Licensed/Unlicensed Spectrum Interoperability in Wireless Mobile Networks. He is also the founder of two journals.